4

Synthesis of High T_c Superconductors

4.1 Synthesis of $Y_1Ba_2Cu_3O_7$ in Bulk Form

Before going into details of preparation, it would be worthwhile to note the undermentioned properties of YBCO system, as these are of relevance in determining the preparation procedure:

1. On heating the Y:123 compound, it decomposes peritectically at about 1,020–1,040°C into Y_2BaCuO_5, CuO and $BaCuO_2$. For this reason, all preparation steps should better be carried out at temperatures below 1,000°C.
2. $Y_1Ba_2Cu_3O_7$ (i.e. orthorhombic phase) is unstable at temperatures higher than 650°C.

At 900–950°C, the oxygen content per formula unit is less then 6.5 and the structure become tetragonal. If quenched in this form, the material is non-superconducting. To regain the oxygen to the desired value (i.e. close to 7), the material should be given a long anneal in O_2 in the temperature range of 400–500°C, to enable the oxygen pick up. Otherwise oxygen can be incorporated by annealing at ∼900°C in flowing oxygen for short durations and then, slow cooling in oxygen atmosphere.

The most widely used method is the conventional ceramic technique, which comprises the following steps:

(1) Weighing the appropriate amounts of starting materials.
(2) Mixing these powders to get a homogeneous mixture.
(3) Calcining the homogeneous mixture to get the reacted material.
(4) Grinding the calcined reacted powder to get the desired particle size.
(5) Shaping the ground powder by pressing (i.e. pelletizing).
(6) Sintering the shaped material.
(7) Annealing in oxygen with a slow cool to get the superconducting material.

The starting materials are Y_2O_3, BaO_2 and CuO. Mixing is done with an agate, mortar and pestle (for small quantities ∼10 gm). For larger quantities, one may use ball mill.

Calcining is carried out in the temperature range of 880–900°C in air. The duration of this calcining can be fixed by intermittent checking of X-ray diffraction for the complete disappearance of the lines due to the reactants. Generally, 10–20 h should be sufficient, but many workers prefer to interrupt the heating, regrind and remix the powder and heat the same again to ensure a total conversion to the desired product.

This is followed by a grinding operation (in a ball mill or mortar and pestle).

The grinding time is such that the final powder becomes approximately micron sized. This powder is then shaped into the desired forms by using a suitable die and punch. The pressure used is generally 5,000 1b in.$^{-2}$.

Sintering is done in an oxygen atmosphere at temperatures around 920–950°C, for a period ranging from a few hours to more than 24 h. The conditions are to be optimized to get as high density as possible.

The sample is then cooled slowly in an atmosphere of flowing oxygen. The rate of cooling is generally maintained at 1–2°C per minute (particularly in the temperature range of 600–400°C). Below 400°C, the sample can be cooled faster.

Platinum crucibles can be used at the calcining stage, if the temperature is lower than 900°C, but at higher temperature, sintering should be done on fused alumina plates (because platinum reacts with the material at temperature >900°C). Other techniques used are sol–gel method and single crystal growth.

The samples so synthesized may be subjected to various characterizations, such as T_c-measurement by Vander Pauw technique, X-ray diffraction, J_c measurement, etc.

4.2 Why Thin Films of High T_c Superconductors?

High T_c superconductivity in the bulk material suffers from low current density, if the current in a sample is increased, a breakdown of superconductivity occurs. Furthermore, since the superconductivity effect is strongly anisotropic in a polycrystalline bulk, an unavoidable averaging of the superconducting properties of all crystal orientations takes place. However, once crystal growth is epitaxial, the super-current density can be increased over that of the poly-crystalline material.

The chemical, mechanical and electrical properties of the available bulk HTSC materials, however, are suitable for only few applications and a great deal of development effect is needed. However, applications involving superconducting thin films, much as hybrid superconducting/semiconducting circuits and microwave/millimetre wave devices seem to be closer in practice than applications of bulk materials.

Thin films are also important in surface studies, nucleation and growth studies, and in the production of meta-stable structures and compositions, consequently these facts necessitate the synthesis of HTSCs in thin film forms.

4.3 Techniques for Thin Film Preparation

The basic steps involved in thin film deposition-techniques are

(a) Creation of material to be deposited in an atomic, molecular or particulate form prior to deposition
(b) Transport of materials, thus, created onto the substrate in the form of vapour, stream or spray
(c) Deposition of material on the substrate and film growth by a nucleation and growth process

The deposition techniques can be distinguished by the way these basic steps are affected. One can, in principle, get films of desired properties by properly modifying these three steps.

The thin film deposition techniques can be broadly classified as physical vapour deposition (PVD) and chemical deposition. The PVD techniques are those in which the first step involves a physical process. In PVD, the thermal energy for the melting and vaporization can be provided by any of the following procedures:

(1) Resistive Heating

This method consists of heating the material with a resistively heated filament or boat, generally made of refractory metals, such as W, Mo, Ta or Nb, with or without ceramic coatings. The choice of the support material is determined by the evaporation temperature and resistance to alloying and/or chemical reaction with evaporant.

(2) Flash Evaporation

A rapid evaporation of a multi-component alloy or compound, which tends to distill fractionally, may be obtained by continuously dropping fine particles of the material onto a hot surface, so that numerous discrete evaporations occur. Alternatively, a mixture of the components in powder form may be fed into the evaporator. The fine powder is fed into a heated Ta or Ir boat by mechanically or ultrasonically agitating the feed chute.

(3) Electron-Beam Methods

The simple resistive heating of an evaporation source suffers from the disadvantages of possible contamination from the support material and the limitations of the input power, which make it difficult to evaporate high melting point materials. These drawbacks are overcome by an efficient source of heating by electron-bombardment of the material.

The simplest electron-bombardment arrangement consists of a heated tungsten filament to supply electrons, which are accelerated by applying a positive potential to the material for evaporating. The electrons lose their energy in the material very rapidly, their range being determined by their energy and the atomic number of the material. Thus, the surface of the material becomes

a molten drop and evaporates. In contrast to this simple work-accelerated e-beam arrangement, one way is to use electron-optics to focus the beam and direct it onto the material for evaporation.

(4) Molecular Beam Epitaxy (MBE)

The deposition of single crystal epitaxial thin films by the condensation of one or more beams of atoms and/or molecules from Knudsen (effusion) sources under ultra-high vacuum conditions is called molecular beam epitaxy (MBE).

The Knudsen effusion source consists of a crucible containing the evaporant, with a small orifice. The orifice dimension is smaller than the mean free path of the vapour in the source cavity and the outflow of the molecules from the source is by effusion. The effusing molecular beam has a large mean free path compared to the source–substrate distance. The flux of the beam is precisely determined by the partial pressures of the vapour species within the chamber, their molecular weight source temperature and orifice dimension. A controlled growth of the film is achieved by the MBE technique.

(5) Sputtering

Sputtering, often described as playing billiard with atoms, is the ejection of target atoms by the impingement of ions from a persistent glow discharge with kinetic energies larger than the binding energy of the target atoms. The surface atoms are sputtered, when the kinetic energy of the incident particles is transferred to the target and the sputtered atoms condense on the substrate to form a thin film.

The process is significantly influenced by the energy and the angle of incidence of the impinging ions and the target material. The sputtering yield, defined as the average number of atoms ejected from the target per incident ion, increases with the increasing energy of ions and their mass (relative to the atomic weight of the target).

(6) Pulsed Laser Deposition (PLD)

Laser deposition is based on the rapid localized heating of a volume of target material determined by the absorption depth of the laser light and the thermal properties of the target. Typically, the combination of energy absorption and heating profile results in the vaporization of the material below the surface of the target leading to the fragmentation and outward projection of a small volume of the surface material. The target material is vaporized in a broad spatial distribution and not in a point-like evaporation.

Using pulsed laser radiation of high intensity, in front of the target surface, a plasma is generated and the vaporized material is ejected in a direct jet-like plasma stream. The forward directed nature of the material ejection results from anisotropic expansion velocities of the atomic species. The physics and chemistry of the whole process is roughly divided into the regime of photon/target interaction at the target site, the regime where the plasma formation and initial isothermal adiabatic expansion takes place, the regime of

the adiabatic expansion, transport, relaxation and interaction with gases in the plasma phase and finally, the condensation on the substrate.

4.3.1 Chemical Deposition Methods

Chemical methods for thin film deposition may be broadly classified in two categories- (1) electroplating and (2) chemical vapour deposition (CVD).

(1) Electroplating or electrodeposition can further be subdivided into (a) Electrolytic deposition, (b) Electroless deposition and (c) Anodic oxidation. Electrolytic deposition utilizes the principles of electrolysis. In electroless deposition, electrolytic action is achieved (without an external potential source) by a chemical reduction process. Electroless deposition is used in the well-known technique of silvering glass dewars. A large number of metals (called "valve" metals) tend to form a protective oxide film of limited thickness, when exposed to oxygen. By anodic polarization of these metals in a suitable aqueous solution (which does not dissolve the oxide), a protective high-resistance film can be grown (Anodic oxidation). The anodization process involves the migration of ions of oxygen, metal or both, depending on the material, through the existing oxide film.

4.3.2 Chemical Vapour Deposition (CVD)

When a volatile compound of the substance to be deposited is vaporized and the vapour is thermally decomposed or reacted with other gases, vapours or liquids at the substrate to yield nonvolatile reaction products, which deposit (in thin film form) on the substrate. The process is called chemical vapour deposition. Due to availability of a large variety of chemical reactions, CVD has been versatile and flexible technique in producing deposits of pure metals, semiconductors and insulators. In CVD, if thermal decomposition of a compound is used to yield a deposit of the stable residue, it is called pyrolysis.

4.3.3 Spray Pyrolysis

In spray pyrolysis, a solution (usually aqueous) containing soluble salts of the constituent atoms of the desired compound is sprayed onto a heated substrate. Every sprayed droplet reaching the hot substrate surface undergoes pyrolytic (endothermic) decomposition and forms a single crystallite, or a cluster of crystallites of the product. The other volatile by-products and the excess solvent escape in the vapour phase. The substrate provides the thermal energy for the thermal decomposition and subsequent recombination of the constituent species, followed by sintering and re-crystallization of the cluster of crystallites. The result is a coherent film. The chemical solution is atomized into a spray of fine droplets by spray-nozzle with the help of a carrier gas, which may or may not play an active role in the pyrolytic reaction involved. The solvent liquid serves to carry the reactants and distribute them uniformly over the substrate area during the spray process.

4.4 Basic Thin film Processes for HTSC Films

Basic processes for the deposition of perovskite thin films are as follows:

1	Amorphous Phase	$T_s < T_{cr}$
2	Polycrystalline	$T_s > T_{cr}$, $T_s < T_{cr}$ and post-annealing
3	Single crystals (On single crystal substrates)	$T_s > T_{epi}$
		$T_s < T_{cr}$ and post-annealing (Solid phase epitaxy)

Thin films of amorphous phase are deposited at the substrate temperature T_s below the crystallizing temperature T_{cr}. The T_{cr} for the perovskite type oxides is 500–600°C. Thin films of polycrystalline phase are deposited at $T_s > T_{cr}$. The polycrystalline phase is also achieved by the deposition of the amorphous phase followed by post-annealing at the annealing temperature above T_{cr}.

Thin films of single crystalline phase are epitaxially deposited on a single crystal substrate at the substrate temperature above an epitaxial temperature T_e ($T_e \geq T_{cr}$). The amorphous thin films deposited on the single crystal substrate will be converted into the (single) crystalline thin films, after the post-annealing at annealing temperature above T_e owing to a solid phase epitaxy.

Various experiments carried out for the deposition of the high T_c thin films are classified into three as indicated in Table 4.1.

The process for the ceramics is composed of three stages: (1) mixing, (2) annealing for crystallization and sintering, (3) annealing for the control of oxygen vacancies.

For the thin films, three processes are considered. The process (1) is deposition at a low substrate temperature followed by the post annealing. This

Table 4.1. Fabrication processes for the high T_c superconductive ceramics and thin films

		Chemical composition	Crystallization	Oxygen vacancy control
Ceramics		Mixing	Sintering 850°–950°C	Annealing[a] 850°–950°C
Thin films	1	Deposition ($T_s < T_{cr}$)	Annealing 850°–950°C	Annealing[a] 850°–950°C
	2	Deposition ($T_s > T_{cr}$)		Annealing[a] 600°–950°C
	3	Deposition ($T_s > T_{cr}$)[b]		

T_s is substrate temperature during deposition, T_{cr} is crystallizing temperature (500–600°C)
[a]slow cooling
[b]quenching

Table 4.2. Fermi energy in 10^5-cal. mole^{-1} at 1190 K for various simple oxides

Y_2O_3	BeO	MgO	ZrO_2	Al_2O_3	SiO_2
1.11	1.15	1.12	1.04	1.03	0.79

process is commonly used for the deposition of the high T_c superconducting thin films, since the stoichiometric composition of the thin films is easily achieved. However, the resultant films are polycrystalline. The single crystal films are possibly obtained by a vapour-phase epitaxy achieved in the process (2) and (3).

Lowering the synthesis temperature is much important not only for scientific interests but also for the fabrication of the thin film superconducting devices. The maximum temperature in the process (2) is governed by the post-annealing process for the control of oxygen-vacancies, however, the oxygen vacancies control will be attained at lower temperature, when the vacancies control is conducted by an oxygen-ion bombardment on the film surface during the film-growth. The structural analyses for the YBCO ceramics suggest that the structural transition from the non-superconducting tetragonal phase into the superconducting orthorhombic phase occurs around 600–700°C. If the substrate temperature during the deposition T_s satisfies the relation

$$T_e \leq T_s \leq T_t,$$

where T_e denotes the epitaxial temperature and T_t, the transition temperature from tetragonal to the orthorhombic phase and if enough oxygen is supplied onto the film surface, during the deposition so as to oxidize the deposited films, the as sputtered films show single crystal phase and reasonably exhibit superconductivity without the post-annealing process through in situ process, which is characterized in process (3).

In the case of the metallic atoms of YBCO, computation shows that in the range of $1{,}100 - 1{,}300$°K, the largest E_F is due to Y_2O_3. Table 4.2 shows E_F in 10^5 −cal. mole^{-1} at 1,190 K for Y_2O_3 and various simple oxides.

From this table, one can infer that BeO and MgO, whose E_F are larger than E_F for Y_2O_3 could be good substrates for YBCO films [1].

Thin film growth techniques can be broadly classified into the following two undermentioned categories:

Those requiring high temperature, post-deposition annealing (Ex-situ annealing)	Film is grown in correct crystalline form during growth (in-situ techniques)
1. The crucial growth step takes place after deposition, i.e. during annealing	1. Although, some low temperature annealing may be required to achieve correct oxygen stoichiometry, but it requires no substantial rearrangement of the lattice after growth:

(*continued*)

(continued)

The film crystallizes by a solid state re-growth mechanism to form a polycrystalline but epitaxial layer	
2. The actual technique used to deposit the layer is of only secondary importance because the crucial growth step takes place long after deposition	2. Advantages: (a) Lower temperatures involved minimize contamination from the substrate (b) single crystal films can be grown with improved physical properties (c) film surface can be smooth
3. All the known HTSCs can be grown by processes involving ex-situ annealing All the reported films with $T_c > 100$ K have been made by careful ex-situ annealing	3. BSCCO and TBCCO are very difficult to be prepared by in-situ technique

4.5 Various Techniques for Deposition of Films of High Temperature Superconductors

The synthesis of high T_c thin films involves the problem of the deposition of a large number (three to five, for the different compounds) of metallic constituents in a fairly well controlled manner as well as the crystallization in the correct structure and the oxygenation for the desired doping of holes. Hence, due to the complexity of the HTSCs with respect to the number of constituents and oxygen stoichiometry, their preparation as epitaxial films was a certain challenge for the scientists in various disciplines. It was barely a few months after the discovery of superconductivity above 77K that the first films of these complex multi-element materials were prepared [2]. This was accomplished first by multi-element deposition techniques. Later, other techniques, such as multisource electron beam evaporation, MBE (molecular beam epitaxy), sputtering, laser ablation, chemical vapour deposition and spray-pyrolysis etc. were used efficiently for the synthesis of high quality HTSC films on a variety of substrates.

The various routes to high T_c thin films differ in the substrate temperature during deposition (T_s), or in other terms, whether the original film is grown in the form of amorphous or micro-crystalline ($T_s < 500°C$) or directly in the tetragonal high resistance phase ($T_s > 600°C$), which converts into the superconducting orthorhombic phase during cooling in an oxygen atmosphere.

Table 4.3. Flow chart for high T_c superconducting thin film preparation

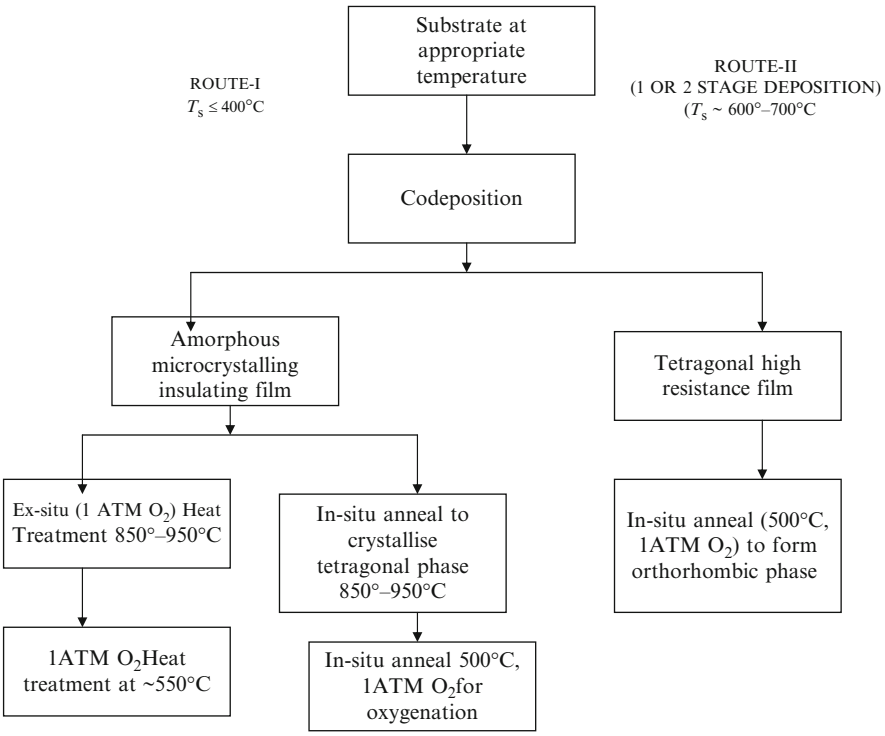

The former processes are termed as ex-situ, whereas the latter ones are in-situ techniques. Table 4.3 shows a flow chart of different preparation routes. Crystallization and oxygenation in the ex-situ techniques can be accomplished by different means, such as furnace annealing, rapid thermal annealing (RTA), or low energy plasma processing for the oxygenation [3]. All these techniques have some specialized advantages, such as low thermal budget for the TA process and this minimized substrate film interaction. The heat treatment leads to an epitaxial growth starting from the substrate/film interface. Apart from the deleterious film/substrate interaction, another disadvantage of route I is the sensitivity of the film properties to complicated processing sequence for crystallization and oxidation. This results in films with low T_c and J_c.

The alternative approach of route II yields an in-situ crystallization in the tetragonal phase, which upon cooling in oxygen converts to the superconducting orthorhombic phase. Here, epitaxial growth can be achieved directly, and films show superior qualities such as high T_c and sharp transition, high J_c and low surface resistance.

4.6 Preparation of Thin Films of HTSC-$YBa_2Cu_3O_{7-x}$: An Introduction

The announcement of superconductivity above 30 K in the La–Ba–Cu–O system by Bednorz and Muller and the subsequent discovery of Y–Ba–Cu–O superconductor by Wu et al. spurred the scientists world over to make an unprecedented effort to explore both the physical mechanism underlying this phenomenon and its obvious technological potential. From both viewpoints, the preparation of the superconducting films was an important step. In the beginning, the preparation of the bulk superconducting oxide samples, using conventional ceramic techniques (grinding, firing and pelletizing), became well established and was reproduced by many researchers. One drawback of the polycrystalline versions in which HTSCs were initially synthesized was low critical current density (J_c), which was about 10^2–10^3 A cm^{-2}. The usual magnitudes of J_c which, for example, is achievable from conventional superconductors is about 10^6 A cm^{-2}. Such a value would be useful for most of the devices, particularly high current ones, like high field electromagnets, lossless transmission, levitating vehicles, MRI etc. At the early stage, it was recognized that low J_c values were due to weak-link effects arising from the presence of high angle grain boundaries separating adjacent gains and also because of absence of suitable flux pinning centres within the grains. Since thin films are necessarily grown on substrates, by proper choice of substrates suitably oriented films without high angle grain boundaries could be prepared and since thin film formation is like vapour quenching, secondary phase forming flux pinning centres might get nucleated. Therefore, formation of thin films of HTSC materials held considerable promise. However, preparing thin films of these materials turned out to be a more difficult task. The first successful deposition using sputtering, from bulk materials, was reported for the ∼40 K superconductors [4,5], including the preparation of microcrystalline thin films [6].

The first report on the formation of thin films of Y–Ba–Cu–O was through electron beam evaporation of individual ingredients by Chaudhari et al. [7]. Later on, other techniques like screen printing, on beam sputtering [8] and pulsed laser evaporation [9] were employed for the synthesis of thin films of these YBCO HTSCs.

4.6.1 Choice of the Substrate for Thin Film Deposition

An ideal substrate should be

(1) Chemically non-contaminating
(2) Having good lattice and thermal expansion match to the film within 5%
(3) Cheap in large size single crystals
(4) Having low dielectric constant and loss
(5) Easily cut and polished

Table 4.4. Some selected substrate materials for deposition of high T_c superconductor films

Material	Structure	Lattice constants (A^0)	Thermal expansion coefficient (K^{-1})	Dielectric constant
Y–Ba–Cu–O	Orthorhombic	3.88, 3.86, 11.67	15×10^{-6}	–
$SrTiO_3$	Cubic	3.905	10×10^{-6}	180
$Y-ZrO_2$	Cubic	5.16	10×10^{-6}	7.8
MgO	Cubic	4.21	12×10^{-6}	9.7
Si	Cubic	5.43	3×10^{-6}	12
SiO_2	Hexagonal	4.91, 5.394	1×10^{-6}	3.8
Al_2O_3	Hexagonal	4.76, 12.9	6×10^{-6}	10.2
Gadolinium Gallium Garnet	Cubic	12.383	8×10^{-6}	15
$MgAl_2O_4$	Cubic	8.085	8×10^{-6}	–
$LaGaO_3$	Orthorhombic	5.52, 5.49, 7.77	–	27
$LaAlO_3$	Rhombohedral	5.357, 60°6′	10×10^{-6}	15
$LiNbO_3$	Hexagonal	5.15, 13.86	–	–

(6) Able to withstand oxidizing atmosphere involved in the fabrication process. Strontium titanate has been the substrate of choice, since it seems to fulfill the best combination of inertness, thermal expansion and lattice matching. However, it is not a perfectly inert substrate material and its ferroelectric properties could be unsuitable in many applications. Zirconnia (ZrO_2) and MgO have much better inertness, but have poor lattice matching properties. $LaAlO_3$ and $LaGaO_3$ are recently developed substrates with improved lattice matching and dielectric properties. Crystallinity, lattice constants, thermal expansion coefficients and dielectric constant of the substrate are quite critical to the final properties, particularly morphology of the deposited films. Table 4.4 gives some details of the crystal substrates and their properties for cuprate superconductors.

Table 4.5 lists dielectric properties of $LaAlO_3$ and other commonly employed substrates.

4.6.2 YBCO Film/Substrate Interaction

One of the crucial aspects related with the formation of thin films, which decides the viability and the physical properties, e.g. texturing and the related parameter "J_c", depends on the film–substrate interaction effect. In all film depositions, a post-deposition heat treatment is required and it is during this treatment that most of the film substrate interaction takes place. The interaction with substrates can further be divided into three groups:

Table 4.5. Dielectric properties of substrates suitable for deposition of high T_c thin films

Material	Al_2O_3	ZrO_2	$SrTiO_3$	MgO	$LaAlO_3$
Dielectric constant					
at 300 K	9.87	26.1	310	9.1	15.3
at 77 K	9.6	25.4	1900	20.5	15.3
Dielectric loss tangent					
tan δ (300 K)	2×10^{-4}	1.7×10^{-2}	3.2×10^{-2}	2.2×10^{-5}	5.8×10^{-4}
tan δ (77 K)	4.2×10^{-5}	7.5×10^{-3}	5.8×10^{-2}	4.9×10^{-6}	8.3×10^{-5}

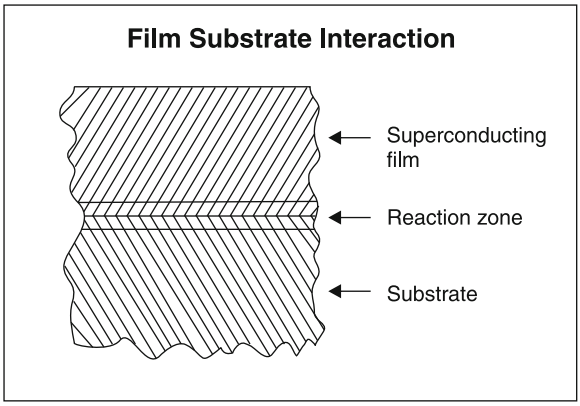

Fig. 4.1. Schematic of the interaction between the $YBa_2Cu_3O_7$ film and the substrate after annealing at ~900°C

1. Reaction between film and substrate
2. Lattice matching
3. Matching of thermal expansion coefficients between the film and substrate

A schematic representation of the interaction between the film and substrate is shown in Fig. 4.1. The film and substrate react at the interface establishing either a reaction zone where new compounds are formed with structures differing from both, the deposit and the substrate, or a zone with a composition gradient where diffusion or inter-diffusion has taken place between the film and the substrate without the formation of new structures. The new zone continues to grow with time and temperature.

Of the substrates that have been used, the best is YSZ (yttria stabilized Zirconia), followed by BaF_2, $SrTiO_3$, MgO, Al_2O_3 in order with Al_2O_3, the worst.

Many studies of YBCO thin films have shown that interdiffusion or reaction can occur with almost all substrate materials including Si, Al_2O_3, $SrTiO_3$, ZrO_2 and MgO [10, 11, 12, 13, 14].

In some cases, the diffusion of small amounts of metal ions from the substrate material into the superconducting YBCO should not cause a prominent decrease in T_c [15]. However, the depletion of elements from YBCO can leave behind non-superconducting material. For most substrate materials, Ba^{2+} ions diffuse most quickly to the substrate film interface, forming a Ba-enriched layer or second Phase. Cu^{2+} ions also tend to diffuse toward the interface. The degree of inter diffusion varies strongly with substrate material and the maximum temperature to which the films are exposed. MgO and Y_2O_3-stabilized cubic ZrO_2(YSZ) seem to be two of the less reactive of the materials mentioned above. YSZ buffer layers have been studied with success as a way of limiting the problem of highly reactive substrate, such as Si and Al_2O_3. Witanachchi et al. [16] have studied the effect of buffer layers on low temperature (i.e. in-situ) growth of mirror- like superconducting thin films of YBCO on sapphire (Al_2O_3), utilizing plasma-assisted laser deposition. Their results are summarized in Table 4.6.

MgO and $BaTiO_3$ improved the value of T_c, while Ag showed a slightly semi-conducting behaviour near T_c. The Ag buffer also improved the normal state resistivity of the YBCO film at room temperature. Optical and scanning electron microscope (SEM) examination showed that the films were mirror-like and very smooth (surface roughness $<0.1\,\mu m$), which is in contrast with the films made by high temperature post-annealing, which showed $>1\,\mu m$ microcrystal structures intercalated in a pseudorandom fashion [17, 18]. The X-ray diffraction (XRD) patterns of the YBCO/$BaTiO_3$/Al_2O_3 showed formation of highly oriented film with *c*-axis perpendicular to the surface. The same results were obtained for the MgO buffer case. The directly deposited film (YBCO/Al_2O_3) was not well oriented and its XRD revealed diffraction peaks other than (001). Thus, the MgO and $BaTiO_3$ buffer layers improved the crystalline structure as well as the J_c of the films.

In the subsequent sections, we proceed to describe the various thin film deposition techniques employed for the synthesis of YBCO superconducting thin films.

Table 4.6. Results for YBCO films using different buffer layers on sapphire substrate

Substrate	Deposition temperature	Buffer layer material (thickness)	T_c	J_c
Al_2O_3	450°C	Plain (no buffer layer)	75 K	4×10^3 (at 40 K)
Al_2O_3	450°C	MgO (500Å)	78 K	9×10^3 (at 40 K)
Al_2O_3	450°C	$BaTiO_3$ (500Å)	83 K	4.5×10^{-4} (at 40 K)
Al_2O_3	450°C	Ag (thickness not known)	75 K	–

4.7 Techniques Employed for Synthesis of YBCO Thin Films

4.7.1 Electron Beam Evaporation

This technique involves the use of thermionically produced electron beams with energies in the range of 5–10 keV, magnetically deflected and focused onto elemental, metallic or alloy or oxide targets located in water cooled holder. The constituents in a complex ceramic composite having different melting points and vapour pressures do not evaporate congruently by this method. In such cases, the deposition of non-stoichiometric films is achieved. This has been observed in the deposition of YBCO high T_c superconducting films by evaporating single phase target of Y–Ba–Cu–O material [19]. Here, the major problem encountered was that the target thermally decomposed into the original and stable oxides, such as CuO, BaO and Y_2O_3 (CuO evaporated first, followed by BaO and Y_2O_3). This resulted in yttrium-deficient films and an extra Y-layer was necessary to achieve the 123 stoichiometry. This problem was significantly overcome by evaporating constituent elements in their respective stoichiometry by precisely controlling the flux of the molecular or atomic beam independently [20]. The schematic view for typical e-beam co-evaporation systems is shown in Fig. 4.2.

Evaporation is usually done in a high vacuum chamber (pressure = 10^{-7} torr). Pure Y and Cu are normally evaporated with electron guns and Ba with an effusion cell [21]. Instead of Ba-metal, which easily oxidizes, inert and easily handled compounds, such as BaF_2, or $BaCO_3$, or BaO or BaO_2 have been used. It is interesting to note that films made from BaF_2 contain only

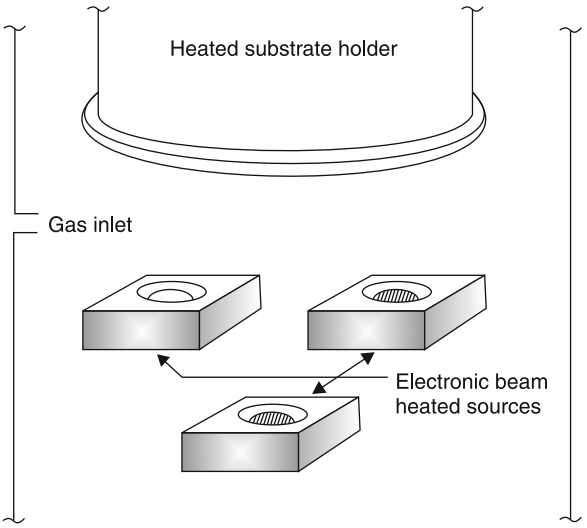

Fig. 4.2. A schematic diagram showing e-beam evaporation process

a small amount of fluorine (<5%), which does not affect the superconducting properties.

Films deposited in ultra-high vacuum from the metal sources were very unstable in air. Exposure to a small partial oxygen pressure $\left(10^{-3}\text{–}10^{-5}\,\text{torr}\right)$ caused oxidation of Y and Ba and improved the stability. However, the as deposited films were sensitive to ambient moisture and immediate annealing in oxygen atmosphere was required to stabilize the film and form the orthorhombic superconducting phase.

The metals have usually been deposited as a set of metallic tri-layers and the layer thickness adjusted so that the desired 123 stoichiometry was obtained. The number and order of the layers vary in different studies, but Cu was generally used for the first layer because it has the lowest oxygen affinity and substrate interactions may, therefore, be minimized. The sequence Ba, Y, Cu has also been used [22].

Substrate temperatures ranging from room temperature to 900°C have been used, the most popular region being 300–500°C. According to Laibowitz [23], film stability is increased at elevated substrate temperatures (450°C). According to Naito [24], the substrate temperature does not significantly affect T_c, but it influences J_c and the shape of R vs T curve. High J_c values were measured on samples deposited at ambient temperature on $SrTiO_3$. The reason for this behaviour lies in the orientation of the 123 phase. With high T_s (∼700–900°C) depositions have random orientations, while at medium T_s (300–500°C) the a-axis is perpendicular to the film. In films deposited at low temperatures, the texture is such that the c-axis is strongly and the a-axis is weakly perpendicular to the substrate. The highest J_c value reported for evaporated films is $10^6\,\text{A}\,\text{cm}^{-2}$ at 81 K.

The microstructure of evaporation deposited 123 films on $SrTiO_3$ depends on the experimental conditions. Naito et al. have explained columnar structure, which indicates the c-axis is oriented perpendicular to the plane of the film.

4.7.2 Molecular Beam Epitaxy

This method has been extensively used for the deposition of epitaxial compound semiconductor thin films. Kwo and co-workers [25] applied this technique for the preparation of ceramic superconductor films. In the case of YBCO deposition, films with 123 stoichiometry have been produced by using metals as source materials. Generally, the three metals are simultaneously deposited by concentrating the vapour fluxes of three sources onto a substrate centrally located with respect to the sources symmetrically distributed on a circular area. The rate of deposition of each is first, individually calibrated, stabilized and subsequently adjusted to yield the desired 123 stoichiometry.

Oxygen was usually introduced to the growing film by a precision leak valve. The base pressures were typically $\leq 2 \times 10^{-10}$ torr. Prior to film growth,

oxygen was blowed into the system and the background pressure increased to 10^{-7} torr. During film growth, the pressure above the film was $\sim 10^{-5}$ torr. The reported growth temperatures vary from ambient to 450°, 530–560° or 600–750°C. The substrates used were (100) Si, $(1\bar{1}02)$ sapphire, (100) yttria stabilized ZrO_2, (100) MgO and (100) and (110) $SrTiO_3$. No superconductivity was observed on Si, while the highest transition temperatures were obtained on $SrTiO_3$ (82 and 89K) and MgO (82K). On (100) $SrTiO_3$, MBE grown 123 films have shown strong orientation (a-axis normal to the surface). With a lower substrate temperatures (300°C), better 123 stoichiometry was obtained with c-axis oriented perpendicular to the film [26, 27]. The c-axis oriented films have a higher degree of structural order, lower normal state resistivity and higher J_c than the a-axis oriented films.

Due to the strong orientation of the MBE grown films, the critical current values measured were high compared to average sputtered or evaporated films. The values are $\sim 10^6\,\mathrm{A\,cm^{-2}}$ at 4.2 K and $> 10^5\,\mathrm{A\,cm^{-2}}$ at 77 K. The requirements for high T_c and J_c values are high purity (no other phases than 123), minimum number of grain-boundaries and high orientation of a-axis perpendicular to the substrate surface. Growth by MBE seems to fulfill these requirements.

4.7.3 Sputter Deposition

Sputtering process is the ejection of individual surface atoms from the solid surface by momentum-transfer from high energy bombarding ions to surface atoms.

The process basically involves a series of nearly elastic collisions between a projectile-atom and target atoms. A projectile atom, typically a noble gas ion (e.g. Ar^+) is accelerated towards the sputtering target. Upon impact with the target, the projectile atom may

(1) Leave the target by scattering (reflecting) backward, and transfer only part of its energy to target atoms, or
(2) Remain embedded (implanted) within the target and so transfer all of its energy to the target. The target atoms, which receive sufficient energy in the direction away from the target (to overcome their binding energy), may leave the target and traverse through the gas phase; these atoms are said to be sputtered. The sputtered atoms will generally re-condense on the first solid surface they come in contact with, and in this manner, a film of the target material will grow, predominantly, atom-by-atom, on surface opposite to the target.

Because of the higher kinetic energy of the sputtered flux, sputter deposited ad-atoms have higher mobilities than do evaporated adatoms, producing better morphologies and microstructures that can be advantageously exploited for superconductor thin film applications. The advantage of sputtering over evaporative methods is that high quality films with good adhesion can be

obtained because, as a result of enhanced mobilities of the adatoms, it would be possible to obtain epitaxial films at much lower substrate temperatures than those obtained by other techniques.

However, its low deposition rate of 20–100Å min^{-1} is its main drawback as long hours of sputtering are required for preparing films of significant thickness. To use it as an effective deposition technique, a large number of incident ions must strike the target per second. The method used to generate the ion-bombardment is the distinguishing feature of the many sputtering techniques utilized. The simplest experimental set up is that of dc-diode sputtering. The ions are generated in a glow discharge plasma, a mixture of neutral gases, ions and electrons sustained by an applied potential (The name "diode" indicates that this is a two electrode discharge: target is the cathode and the substrate platform (or entire chamber) is made the anode). The negative bias applied to the target (typically ∼1,000 V) accelerates incoming positive ions, resulting in sputtering, secondary electron emission and noble gas reflection.

Electrons emitted from the target accelerate away due to the negative potential and may collide with gas atoms, ionizing them. These emitted secondary electrons are then mainly responsible for sustaining the plasma. In order to sustain the plasma, the pressure must be controlled and be well below the atmospheric pressure. Also, the sputtering gas must be very pure to obtain a film of high purity. The chamber is first evacuated to low pressure and then, the required pressure is achieved by flowing the sputtering gas into the system. At this point, the potential is applied to ignite the plasma and begin sputtering. The main parameters describing the sputtering process in this case are

(1) Sputtering pressure
(2) The applied voltage
(3) The sputtering (ion) current at the target

The power applied at the target may be either dc or rf, rf power is necessary when sputtering an insulating target to avoid a charge build up at the surface.

Figure 4.3 illustrates different sputtering configurations.

Other sputtering techniques commonly employed are magnetron sputtering, triode sputtering and ion beam sputtering.

The difference between magnetron and diode sputtering systems is the application of a magnetic field at the target. The magnetic field and the electric field combination very effectively confines electrons enabling more gas to be ionized per electron and so, a higher sputtering current is obtained at a lower sputtering voltage and less secondary electrons will bombard the substrate during film-growth [28].

The magnetron has the advantage of operating with higher deposition rates and with less electron and energetic atom bombardment during growth than in diode system. Because of its good operational stability, it is generally the preferred technique.

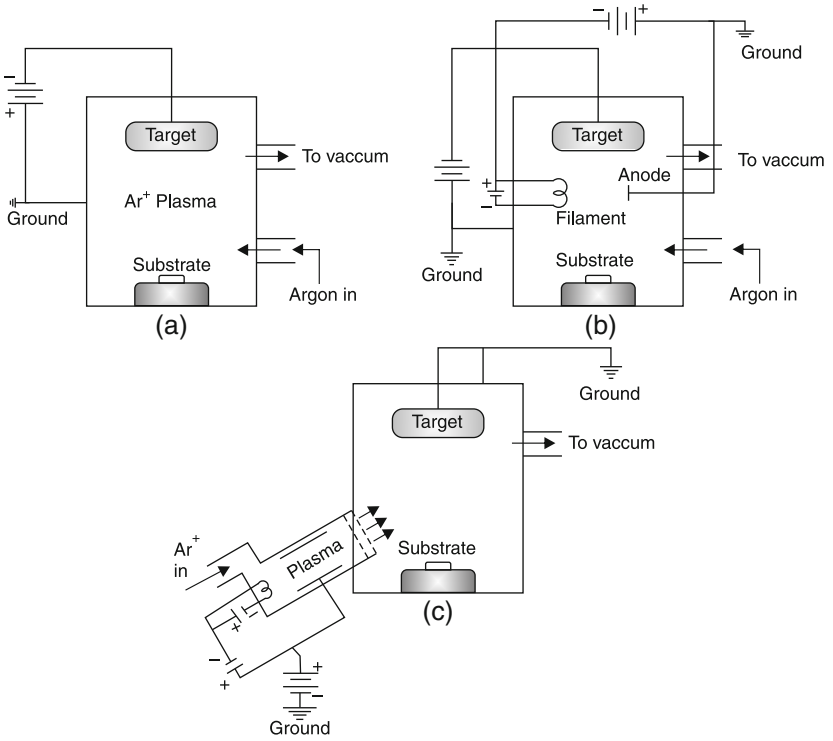

Fig. 4.3. Schematic illustrations of (**a**) Diode sputtering (**b**) Triode sputtering and (**c**) Ion-beam sputtering

In the triode sputtering arrangement, instead of relying on the secondary electrons emitted from the target, to sustain the plasma discharge, a third electrode (typically a hot filament cathode) is used to inject electrons into the plasma. The plasma is then sustained between the hot filament (cathode) and the anode, with the target as the third electrode, which can be biased independently. This allows more control over the process parameters, compared to the diode and magnetron systems. However, the hot filament makes the triode configuration less rugged than the other methods [29].

The ion-beam sputtering technique employs a confined ion-source, which serves to produce the plasma and to accelerate the ions towards the target. In this case, the sputtering parameters are totally independent of the target. The ion beam technique offers the control of the triode system with the advantage that no target-bias is necessary and the energy and direction of the incident ions are better defined [30].

4.7.4 Sputter Deposition of HTSC Films

Sputtering offers certain advantages over other thin film deposition techniques for the growth of high T_c films. Because of the higher kinetic energy of the

sputtered flux, sputter deposited adatoms have higher mobilities than do evaporated adatoms, producing morphologies and microstructures that can be advantageously exploited for superconductor thin film applications. In addition, as a result of the enhanced mobilities of the adatoms, it is possible to obtain epitaxial films at much lower substrate temperatures than those obtainable by other techniques.

The first sputter deposited superconducting thin films were Sr–La–Cu–Oxides, but majority of studies were on the YBCO system [31]. All types of sputtering techniques, including dc diode, dc triode, rf diode, dc magnetron and rf magnetron have been employed in the studies, but rf magnetron sputtering is the most commonly used method. As a sputtering gas usually argon is used, desired chemical reactions of the sputtered atoms/ions in the plasma can be achieved by adding reactive gases to the sputtering gas.

In the case of YBCO and other multi component oxide system, tremendous problems arise from the formation of negatively charged particles at the target (cathode) side. Elements with a large electronegativity difference (e.g. oxygen and the alkaline earth metals) form negative ions, which are accelerated away from the target by the potential difference of the cathode dark space. This energetic particle flux is directed to the substrate in conventional sputtering geometries leading to selective re-sputtering of the growing film, which modifies the film composition or gives rise (in extreme cases), to etching of the substrate rather than deposition. To overcome these problems, following four different routes are used:

(1) To work at gas pressures high enough to reduce the kinetic energy of the ions striking the substrate below the binding energy [32].
(2) To place the substrate off-axis so it will not face the cathode [33].
(3) To design the system for a minimum discharge voltage [34].
(4) To adjust the target composition for a compensation of the re-sputtering effects [35].

Practically, a huge variety of different arrangements of target-substrate position and target configurations have been tried for in situ processes. The sputtering source configurations include multi-target arrangements using metal, metal alloy or metal oxide targets, single ceramic Y:123 targets, single off-stoichiometric YBCO targets and stoichiometric Y:123 hollow cylindrical targets. A comprehensive review covering the developments till 1988 has been given by Leskela [36].

Among several different sputtering techniques, magnetron sputtering offers additional advantages, in that deposition at lower sputtering pressure and target power density is possible. This, in combination with the secondary electron confinement at the target due to the applied magnetic field helps to prevent re-sputtering and heating of the growing film. Figure 4.4 illustrates popularly used magnetron sputtering employing the off-axis geometry first demonstrated by researchers at IBM. Sandstorm et al. [37] have also described the use of single target rf magnetron sputtering in off-axis geometry that has

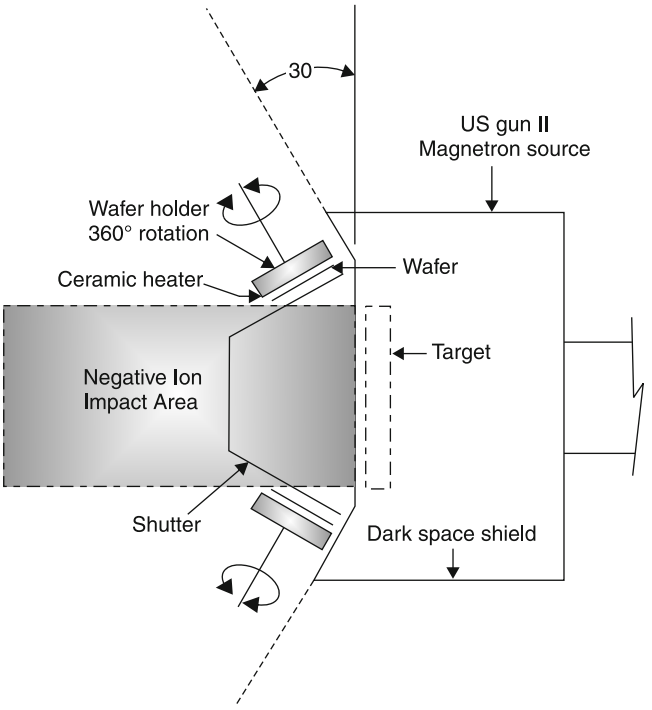

Fig. 4.4. A schematic diagram of off-axis sputtering process

allowed routine production of high T_c $YBa_2Cu_3O_{6+x}$ films from a slightly composition compensated target (+6% Y, −7% Ba).

The $SrTiO_3$ substrates (held at 350°C) are placed outside the region of head-on negative ion flux, but still immersed in the outer edge of the plasma region. Substrate wafers are held on individual heated holders that are rotated to facilitate the achievement of uniform thickness and composition. The sputtering process is carried out in a small chamber evacuated with a $360\,l\,s^{-1}$ turbo pump and having a base pressure of 10^{-7} torr. Typical plasma parameters are 100 W of rf power at 10 MHz, ∼165 V dc self bias with a 98% Ar, 2% O_2 gas flow mixture at 6 m Torr total pressure. Deposition rates are 7–10 nm Min, so that run durations of 40–60 min are required to yield the ∼400 nm thick films. With high temperature (850°C) ex-situ anneals, completely superconducting films (at $T_c \sim 86$–89 K) were obtained. J_c at 77 K ranged from 10^4 to $8 \times 10^5\,A\,cm^{-2}$.

4.7.5 Pulsed Laser Deposition

At present, it is an efficient technique for the preparation of high quality YBCO thin films and is a much faster technique than off-axis sputtering. The first application of pulsed lasers to the deposition of HTSC materials was

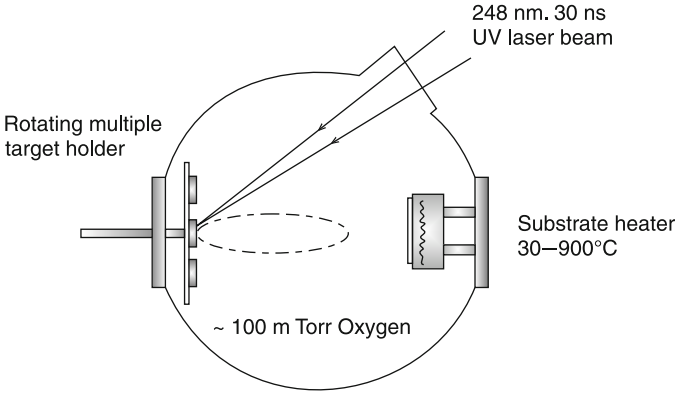

Fig. 4.5. A schematic diagram of experimental set up used in pulsed laser deposition process

demonstrated by the Bellcore- Rutgers group in 1987. Figure 4.5 illustrates schematically the Bellcore- apparatus used for laser deposition. The target, in the form of a pellet (about 2.5 cm in diameter, 6 mm thick) of YBCO, is mounted on a rotating holder in a vacuum chamber with a base pressure of about 2×10^{-7} torr and is irradiated through a quartz window by the output of 1 J pulse^{-1} KrF excimer laser. The targets are rotated during deposition to ensure that the beam always encounters fresh material. A quartz lens is used to forces the beam onto the target to achieve an energy density $\sim$1–2 J cm^{-2}. The substrate is mounted on a heater positioned about 8 cm from the target. Film growth proceeds as material is ablated from the source disk and deposited onto the substrate. The rate of deposition is $\sim$0.2 A° pulse^{-1} at a laser repetition rate of 5 Hz. A typical set of deposition parameters [38] is

Wavelength 248 nm [Kr F]
Energy density 1–2 J cm^{-2}
Target spot size 3 mm^2
Substrate target distance 3–4 cm
Oxygen background pressure 1 m bar
Substrate temperature 780°C

4.7.6 Chemical Vapour Deposition

In this technique, the metal organic compounds are used as the source for the deposition of the oxide thin films. The chemical reaction is initiated at or near the substrate surface, which produces the desired material in the form of thin film. Organic precursor compounds bearing the required metal atoms are heated and an inert gas mixed with oxygen transports the resultant vapours into a reaction vessel containing a heated substrate onto which the deposition occurs (Fig. 4.6).

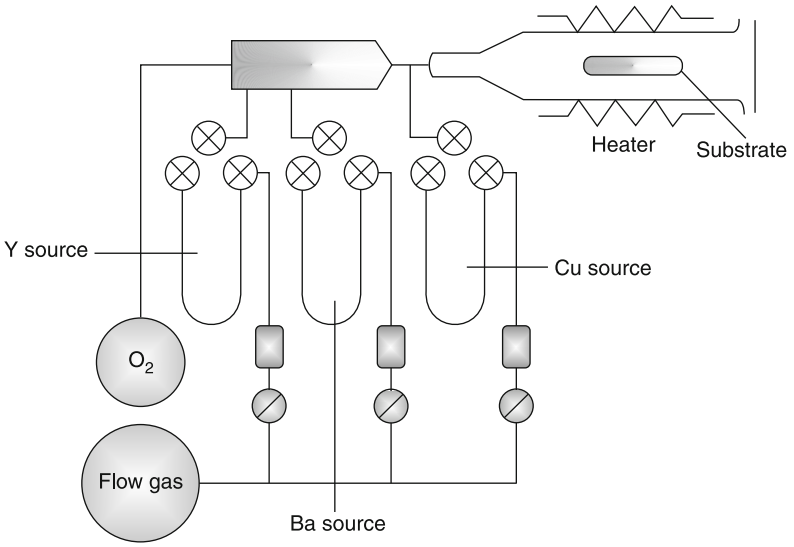

Fig. 4.6. Schematic illustrating metal organic chemical vapour deposition (MOCVD)

One of the few compounds in which both rare-earths and alkaline earths are volatile are β-diketonates, which have been used in gas-phase thin film growth. Berry et al. reported MOCVD growth of Y-123 films using β-diketonates as sources and N_2 as carrier gas. Film growth occurred via depostion of the reactant gases on a MgO substrate surface in an O_2 rich atmosphere. The as-deposited films were amorphous, but a semiconducting film with a T_c of 20 K was obtained after annealing at 890–920°C. The quality of the film could be improved by optimizing the growth conditions.

Yamane et al. [39], Nakamori et al. [40] and Zhang et al. [41], have used the (2, 2, 6, 6-tetramethyl-3, 5-heptanedione) β-diketonate complexes of Y, Ba and Cu as source materials in their CVD experiments. Epitaxially growth films were obtained on (100) $SrTiO_3$ and yttria stabilized ZrO_2 at substrate temperatures of 650 and 900°C. Oxidation was performed in situ after the deposition and T_c and J_c values of 84 K and 2×10^4 A cm^{-2} (at 77 K) respectively were measured.

References

1. P. Bernstein et al., Physica C **162–164**, 611 (1989)
2. R.B. Laibowitz et al., Phys. Rev. **B 36**, 4047 (1987)
3. I. Tarasaki et al., Jpn. J. Appl. Phys. **27**, L1480 (1988)
4. M. Kawasaki et al., Jpn. J. Appl. Phys. **26**, L 388 (1987)
5. N. Terada et al., Jpn. J. Appl. Phys. **26**, L 508 (1987)
6. M. Suzuki, T. Murakami, Jpn. J. Appl. Phys. **26**, L 524 (1987)

7. P. Chaudhuri et al., Phys. Rev. Lett. **58**, 2684 (1987)
8. P.N. Kobrin et al., Adv. Cer. Mater. (Special issue) **38**, 430 (1987)
9. D. Dijkkamp, T. Venkatesan et al., Appl. Phys. Lett. **51**, 619 (1987)
10. M. Naito et al., J. Mater. Res. **2**, 713 (1987)
11. Y. Enomoto et al., Jpn. J. Appl. Phys. **26**, L 1248 (1987)
12. D.M. Hwang et al., Appl. Phys. Lett. **52**, 1834 (1988)
13. T. Venkatesan et al., J. Appl. Phys. **63**, 4591 (1988)
14. H. Nakajima et al., Appl. Phys. Lett. **53**, 1437 (1988)
15. M.F. Yan et al., J. Appl. Phys. **63**, 821 (1988)
16. Witanachchi et al., Appl. Phys. Lett. **55**(3), 295 (1989)
17. R.P. Gupta et al., Appl. Phys. Lett. **52**, 1987 (1988)
18. J.V. Mantese et al., Appl. Phys. Lett. **52**, 1741 (1988)
19. V. Matijasevic et al., J. Mater. Res. **6**(4), 682 (1991)
20. H.U. Habermeier et al., J. Less Common Metals **151**, 257 (1989)
21. AJ.G. Schellingerhout et al., Z. Phys. **B 71**, 1 (1988)
22. C.X. Qui, I. Shin, Appl. Phys. Lett. **52,** 587 (1988)
23. R.B. Laibowitz et al., Phys. Rev. **B 35**, 8821 (1987)
24. M. Naito et al., J. Mater. Res. **2**, 713 (1987)
25. J. Kwo et al., Phys. Rev. B. **36,** 4039 (1987)
26. C. Webb et al., Appl Phys. Lett. **51**, 1191 (1987)
27. J. Kwo et al., Mater. Res. Soc. Proc. **99**, 339 (1988) ed. by MB Brodsky et al., Pittsburgh
28. J.L. Vossen, J.J. Cuomo in *Thin Film Processes*, ed. by J.L. Vossen, W. Kern (Academic, Orlando, 1978)
29. T.C. Tisone, P.D. Cruzon, J. Vac. Sci. Technol. **12,** 1058 (1975)
30. H.R. Kaufman, *Fundamentals of Ion Source Operation* (Common wealth Scientific Corporation, Alexandria, 1984)
31. Z.L. Bao et al., Appl. Phys. Lett. **51**, 946 (1987)
32. U. Poppu et al., Solid State Commun. **66**, 661 (1988)
33. H.C. Li et al., Appl. Phys. Lett. (1988)
34. G.K. Wehner et al., Appl. Phys. Lett. **52**, 1187 (1988)
35. S.M. Rossnagel, J.J. Cuomo, AIP Conf. Proc. **165**, 106 (1987)
36. M. Leskela et al., J. Vac. Sci. Technol. **A7**, 3147 (1989)
37. R.L. Sandstrom et al., Appl. Phys. Lett. **53,** 444 (1988)
38. H.U. Habermeir et al., Physica C **180**, 17–25 (1991)
39. H. Yamane et al., Appl. Phys. Lett. **53**, 1548 (1988)
40. T. Nakamori et al., Jpn. J. Appl. Phys. **27**, L1265 (1988)
41. K. Zhang et al., Appl. Phys. Lett. **54**, 380 (1989)